



AECL-11240

**A UV Pre-Ionized Dual-Wavelength Short-Pulse  
High-Power CO<sub>2</sub> Laser Facility for Laser Particle  
Acceleration Research**

**Laser CO<sub>2</sub> de grande puissance, à impulsion courte, à  
double longueur d'onde, pré-ionisé à l'UV pour la  
recherche sur l'accélération des particules au laser**

N.A. Ebrahim, J.F. Mouris, R.W. Davis

AECL Research

**A UV PRE-IONIZED DUAL-WAVELENGTH SHORT-PULSE HIGH-POWER CO<sub>2</sub> LASER  
FACILITY FOR LASER PARTICLE ACCELERATION RESEARCH**

N.A. Ebrahim, J.F. Mouris and R.W. Davis

Accelerator Physics Branch  
Chalk River Laboratories  
Chalk River, Ontario K0J 1J0  
1994 December

AECL-11240

**EACL Recherche**

**LASER CO<sub>2</sub> DE GRANDE PUISSANCE, À IMPULSION COURTE,  
À DOUBLE LONGUEUR D'ONDE, PRÉ-IONISÉ À L'UV  
POUR LA RECHERCHE SUR L'ACCÉLÉRATION  
DES PARTICULES AU LASER**

par

N.A. Ebrahim, J.F. Mouris et R.W. Davis

**RÉSUMÉ**

Nous décrivons dans ce rapport l'appareil au laser CO<sub>2</sub> de grande puissance, monomode, à impulsion courte et à double longueur d'onde de Chalk River utilisé pour la recherche sur l'accélération des particules au laser et sur les modifications du matériel CANDU®. L'appareil est construit autour des modules de décharge laser CO<sub>2</sub> de Lumonics Inc., à excitation transversale à pression atmosphérique, pré-ionisé à l'UV, pour lesquels il a été conçu. Des pics de puissance volumique focalisée de  $2 \times 10^{14}$  W/cm<sup>2</sup> ont été obtenus à des impulsions de 500 picosecondes.

Physique des accélérateurs  
Laboratoires de Chalk River  
Chalk River (Ontario) K0J 1J0

Décembre 1994

AECL-11240

## **AECL Research**

### **A UV PRE-IONIZED DUAL-WAVELENGTH SHORT-PULSE HIGH-POWER CO<sub>2</sub> LASER FACILITY FOR LASER PARTICLE ACCELERATION RESEARCH**

N.A. Ebrahim, J.F. Mouris and R.W. Davis

#### **ABSTRACT**

In this report we describe the Chalk River dual-wavelength, short-pulse, single-mode, high-power CO<sub>2</sub> laser facility for research in laser particle acceleration and CANDU® materials modifications. The facility is designed and built around UV-preionized transversely-excited atmospheric-pressure (TEA) Lumonics CO<sub>2</sub> laser discharge modules. Peak focussed power densities of up to  $2 \times 10^{14}$  W/cm<sup>2</sup> in 500 ps pulses have been obtained.

Accelerator Physics Branch  
Chalk River Laboratories  
Chalk River, Ontario K0J 1J0  
1994 December

AECL-11240

## I. INTRODUCTION

The concept of using lasers and plasmas for the acceleration of particle beams is revolutionary in accelerator science. One of the main attractions of such concepts is the significantly higher accelerating field gradients that have been predicted by theory and particle simulations. One such concept is that the laser plasma beatwave accelerator concept: relativistic, large-amplitude electron plasma waves are generated by the non-linear coupling of two intense laser beams of slightly different frequencies propagating through a low-density plasma.<sup>1</sup> If the difference frequency of the lasers is chosen to match the plasma frequency, the ponderomotive force of the beatwave can resonantly build up the relativistic plasma wave. A trailing, relativistic electron bunch injected into the potential well of the plasma wave at the appropriate phase remains synchronized to the wave and accelerated for a significant period of time.<sup>2</sup> Complex and sophisticated experiments are required to test theoretical predictions and explore the implications of these ideas for useful ultra-high-energy particle accelerators<sup>3-6</sup> An essential element of such an experimental facility is a high-power laser system. For the laser plasma beatwave concept, the laser output must consist of two wavelengths in a single longitudinal and transverse mode, which must be synchronized. Furthermore, the laser pulselength must be short ( $\sim 500$  ps) with a fast risetime, that matches the linear growth of the plasma wave amplitude. A final requirement is that the focussed laser power density must be of the order of  $10^{14}$  W/cm<sup>2</sup> in order to create large-scale, high-density, homogeneous plasmas via tunnelling ionization of hydrogen gas and, generate plasma waves of interesting amplitudes.

The peak focussed power density of up to  $2 \times 10^{14}$  watts/cm<sup>2</sup> can also be used to drive shock waves in solids. Laser-shock surface treatment is expected to harden materials, thus improving their fatigue and fretting-fatigue resistance. Preliminary experiments of surface hardening of Zr-2.5Nb CANDU® pressure-tube specimens by shock waves generated by the focussed CO<sub>2</sub> laser beam have already been performed. The high peak power laser beam can also be used to deposit diamond-like films on CANDU pressure-tube samples, to improve the fretting-wear resistance of Zr-2.5Nb CANDU pressure tubes, because of the diamond's high hardness and low coefficient of friction. The basic idea is to produce a hot (250-300 eV) high-density ( $> 10^{19}$  cm<sup>-3</sup>) plasma on a carbon target containing highly-stripped ions (C<sup>+6</sup>) with a high-irradiance laser beam in a high-vacuum chamber, and deposit those ions on a cool Zr-2.5Nb specimen. This is expected to produce a diamond-like, thin-film that has a hardness approximately half that of diamonds. Experiments have been designed to test these ideas using the high-power CO<sub>2</sub> laser facility.

In this report we describe the UV-preionized, short-pulse, high-power, single-mode, simultaneous dual-wavelength CO<sub>2</sub> laser system at Chalk River.

## II. THE CO<sub>2</sub> LASER FACILITY

The basic philosophy in the design of the CO<sub>2</sub> laser facility was to construct a compact system around a series of UV-preionized, transversely-excited, high-pressure, Lumonics laser discharge modules. The dual-wavelength emission is produced in spatially separated cavities in a common discharge of the oscillator. In normal operation, the output of the oscillator is a gain-switched pulse with a duration of approximately 100 ns and typical pulse energies of 200-300 mJ. Since the gain width (approximately 4 GHz per atmosphere of laser gas mixture) in a high-pressure discharge is very large compared to the mode spacing ( $\Delta\nu = c/2 L$ , or approximately 0.15 GHz for a 1 m resonator), the laser gain is essentially constant over a number of modes, as is the spontaneous emission rate. Hence, the output exhibits strong modulation, which results from the beating between different cavity modes that grows from spontaneous emission. Single longitudinal mode operation is obtained by incorporating a low-pressure laser section and a diffraction grating in each cavity.<sup>7</sup> Single transverse mode operation is attained by locating an intra-

cavity aperture near the diffraction grating. A 500 ps pulse, sliced from the oscillator output by three Pockels cells operated in tandem, is amplified to a 100-150 mJ level by making four passes through the gain medium in a Lumonics 820 discharge module. This short pulse is then amplified to the final 50-60 J level by triple-passing the low-energy pulse in a high-pressure Lumonics 612 amplifier.

### III. LOW-ENERGY HYBRID-OSCILLATOR DRIVER

The layout of the low-energy short-pulse driver for the CO<sub>2</sub> laser facility is shown schematically in Figure 1. For simultaneous dual-wavelength operation it is essential that the two emissions be independently tunable, free from gain-competition effects, and well synchronized in time. Gross jitter problems are eliminated by using a common electrical discharge in the oscillator for the two cavities. The oscillator in this facility is a UV-preionized, transversely-excited, atmospheric-pressure, (TEA) Lumonics 821 HP CO<sub>2</sub> laser with an active discharge length of 48 cm and a clear aperture of 3.3 cm×2.8 cm. The two cavities are spatially separated to avoid gain competition. The variable delay in the two emissions, which arises from the different gains of the corresponding rotational lines, is compensated for by two, separate quasi-cw, low-pressure, gain sections, which allow a control of the pulse buildup time by varying the low-pressure section parameters.<sup>8</sup> Furthermore, the hybrid configuration allows the operation of both cavities in single longitudinal and transverse modes, resulting in smooth temporal and spatial pulse shapes.

The two low-pressure discharge tubes are identical in construction, with an active length of 60 cm and a bore diameter of 1.5 cm. The plasma tubes are operated with a trigger-transformer-delay unit (TTD) in conjunction with an auto-ignition coil, high-voltage pulse transformer. The low-pressure sections are timed to fire approximately 650 μs before the main TEA discharge, and are operated at pressures between 3 and 12 torr, with premixed gas, with the CO<sub>2</sub>:N<sub>2</sub>:He ratio of 10:10:80 flowing continuously through the tubes. Both the main oscillator and the low-pressure tubes are sealed with anti-reflection-coated NaCl windows at Brewster's angle. The two cavities are formed with Littrow-mounted, blazed gratings at one end and dielectric-coated, 60% reflectivity, 20-m radius-of-curvature germanium mirrors at the output end. The output mirrors are mounted on piezoelectric transducers (PZT's) to give fine control of cavity lengths. Adjustable intracavity apertures near the gratings are used to achieve the lowest transverse-mode operation. The two cavities are 2.7 m long, with the corresponding longitudinal-mode spacing of approximately  $\Delta\nu = c/2L \approx 55$  MHz. Figure 2 shows photographs of the oscilloscope traces of the signal for emissions on the 10P(20) line at 10.59 μm and 10R(20) at 10.25 μm, recorded simultaneously using a photon-drag detector. In Figure 2a the low-pressure discharge in the 10R(20) cavity (the second signal) is turned off, to show the characteristic self-mode-locked structure. The dual-cavity hybrid CO<sub>2</sub> oscillator produces 200-300 mJ, 100 ns, single longitudinal and transverse mode pulses tuned to the 10P(20) transition at 10.59 μm and 10R(20) transition at 10.25 μm. By adjusting the premix pressures in the plasma tubes, the pulse buildup time can be varied to synchronize the emissions from the two cavities, as shown in Figure 2b. Collinear propagation of the two beams is obtained by transmitting the beams through an anti-reflection-coated NaCl prism at the appropriate angles of incidence, so that the emerging beams overlap and are collinear. Figure 3a shows a typical signature of the oscillator beam recorded as a "burn-mark" on a sheet of unexposed polaroid film.

### IV. ULTRAFAST ELECTRO-OPTIC SWITCHING SYSTEM

A variable-width pulse is sliced from the hybrid oscillator pulse by two, 15 mm aperture, GaAs Pockels cells operated in tandem.<sup>9</sup> The transmission of each Pockels cell is given by

where  $V(t)$  is the applied voltage waveform and  $V_{\lambda/2}$  is the half-wave voltage given by

$$V_{\lambda/2} = \frac{\lambda_0}{2n^3 r_{41}} \frac{d}{l}, \quad (1)$$

$$T = \sin^2 \left( \frac{\pi}{2} \frac{V(t)}{V_{\lambda/2}} \right), \quad (2)$$

where  $\lambda_0$  is the vacuum wavelength of the radiation,  $n$  is the index of refraction of the electro-optical material,  $r_{41}$  is the electro-optic coefficient, and  $d/l$  is the aspect ratio of the crystal. For  $\lambda_0 = 9.3 \mu\text{m}$ ,  $n = 3.21$ ,  $r_{41} = 1.6 \times 10^{-12} \text{ m/V}$ ,  $d = 15 \text{ mm}$ ,  $l = 65 \text{ mm}$ , the half-wave voltage  $V_{\lambda/2} = 23 \text{ kV}$ .

The GaAs crystals are mounted in impedance-matched transmission-type holders of the Los Alamos design,<sup>9</sup> and a 3 ns, 23 kV half-wave pulse is applied from a high-pressure (160 psig  $\text{N}_2$ ), laser-triggered, spark gap (LTSG). The 10  $\mu\text{m}$  switching is nearly 100% efficient. Typically, the final pulse width after the third germanium polarizer (P3) is just the difference between the electrical delay ( $T_E$ ) and the optical delay ( $T_o$ ) between the Pockels cells, PC1 and PC2. The minimum pulse half-width possible from this system is just one half the LTSG risetime. The schematic of the laser-triggered spark-gap is shown in Figure 4.

## V. PRE-AMPLIFIER SYSTEM

The approximately 1 mJ pulse from the hybrid oscillator-switchout system is amplified to a 100-150 mJ level by four passes through a Lumonics 821 HP UV-preionized, 2 atm preamplifier. Spatial filtering is achieved by means of apertures A21, A22 and A23 (Figure 1), and produces a high-quality output beam, with a measured power-contrast ratio of better than  $5 \times 10^3 : 1$  after the preamplifier. Figure 3b shows a typical "burn-mark" of the pre-amplifier beam recorded on a sheet of unexposed polaroid film.

## VI. HIGH-PRESSURE AMPLIFIER

The short pulse is amplified in a 3 atm, large-aperture Lumonics 612 high pressure-amplifier.<sup>10</sup> In order to extract the stored energy efficiently, the amplifier is used in a triple-pass configuration, with the optical components and the discharge housed in a common enclosure (Figure 5). The 1 cm diameter driver beam is focused before entering the gain medium, and expands to approximately a 5 cm diameter at the end of the first pass. The beam is then reflected through the discharge to the final pass collimating mirror, where it is apertured to an 8 cm diameter before completing the third pass. A 1 cm thick, saturable, absorber cell inserted in front of the second pass return mirror makes the system stable to parasitic oscillations, provided that the cell contains a partial pressure of at least 3 torr of  $\text{SF}_6$ .

The 11 cm diameter beam from the final amplifier, containing 50 J at 10.59  $\mu\text{m}$  and 10 J at 10.25  $\mu\text{m}$ , is focused into the interaction chamber (Figure 6) by an off-axis parabolic mirror to a near-diffraction-limited spot with a diameter of approximately 250  $\mu\text{m}$ , to yield a peak intensity in vacuum of  $2 \times 10^{14} \text{ W/cm}^2$ . These two wavelengths correspond to a resonant plasma density of  $1 \times 10^{16} \text{ cm}^{-3}$ . The laser pulsewidth is approximately 500 ps full-width at half-maximum (FWHM), with a linear risetime of

approximately 200 ps. Figure 3c shows the "burn-mark" from the high-energy laser beam as recorded on a sheet of unexposed polaroid before it enters the focussing chamber (Figure 6).

## VII. MASTER TIMING GENERATOR

Figure 7 shows a schematic of the master timing generator, which provides the timed trigger pulses to synchronize the different laser discharges and provide the appropriate timing for the pulse to be amplified in the laser chain. A pulse generator running at 1 Hz provides a trigger pulse that fires the two low-pressure laser sections approximately 650  $\mu$ s before the oscillator discharge. The delays 'A' and 'B' to the low-pressure sections are optimized for best smoothing. The delay between the oscillator and pre-amplifier firings is also adjusted for maximum output power from the pre-amplifier. The delay in firing the high-pressure amplifier is adjusted with respect to the monitor pulse from the laser-triggered spark-gap to maximize the energy from the amplifier. Two other delayed pulses are generated from this system: one to trigger the magnetron system for the linear accelerator, and the other pulse from the laser-triggered spark-gap, with a suitable delay, to fire the electron gun on the linear accelerator. This allows the synchronization of the laser pulse with the electron pulse from the linear accelerator. The 23 kV, half-wave pulse from the laser-triggered spark gap propagates through the three Pockels cells and is terminated in a 50  $\Omega$ , high-voltage terminator (Figure 8) to minimize reflections in the transmission line. A voltage divider provides a series of trigger pulses which are synchronized to the oscillator pulse to better than 100 ps. These pulses are used to synchronize the various components in the laser chain, the accelerator system and the experimental systems. The master timing generator is battery-powered and has electro-optic isolation, to reduce electrical interference and ground loops.

## VIII. OFF-AXIS PARABOLIC FOCUSING SYSTEM

The 10-cm diameter laser beam is focussed with an off-axis, diamond-turned parabola located inside the focussing vacuum chamber (Figure 9). The use of reflective optics and parallel windows in the laser chain, as well as reflective focussing optics, ensures that good collinearity of the two wavelengths is maintained and that the two wavelengths are brought to a focus at the same point in the target chamber.

The off-axis, parabolic-focussing mirror has a diameter of 15 cm, effective focal length of 125 cm, off-axis distance of 22.23 cm and off-axis angle of 10.15 degrees. The mirror was fabricated from solid aluminium (Aluminium 6061 T6), turned on a diamond lathe and coated with chromium and gold. During the machining process, a 12.7 mm flat reference face was machined normal to the optical axis so that the optical axis could be located precisely using an auto-collimator. The best focal position is located by shifting the auto-collimator beam to the centre of the mirror, locating a pinhole in the centre of the target chamber and determining the best focus for the pinhole.

With an f-number of 12.5, the focussing mirror was designed to produce a focal spot of diameter approximately 250  $\mu$ m and a focal depth of approximately 15 mm. The focal power density of the beam is then expected to approach  $2 \times 10^{14}$  W/cm<sup>2</sup>. This has been confirmed in experiments, where plasmas have been produced by the tunnelling ionization of hydrogen gas, which has a tunnelling ionization threshold of  $2 \times 10^{14}$  W/cm<sup>2</sup>.



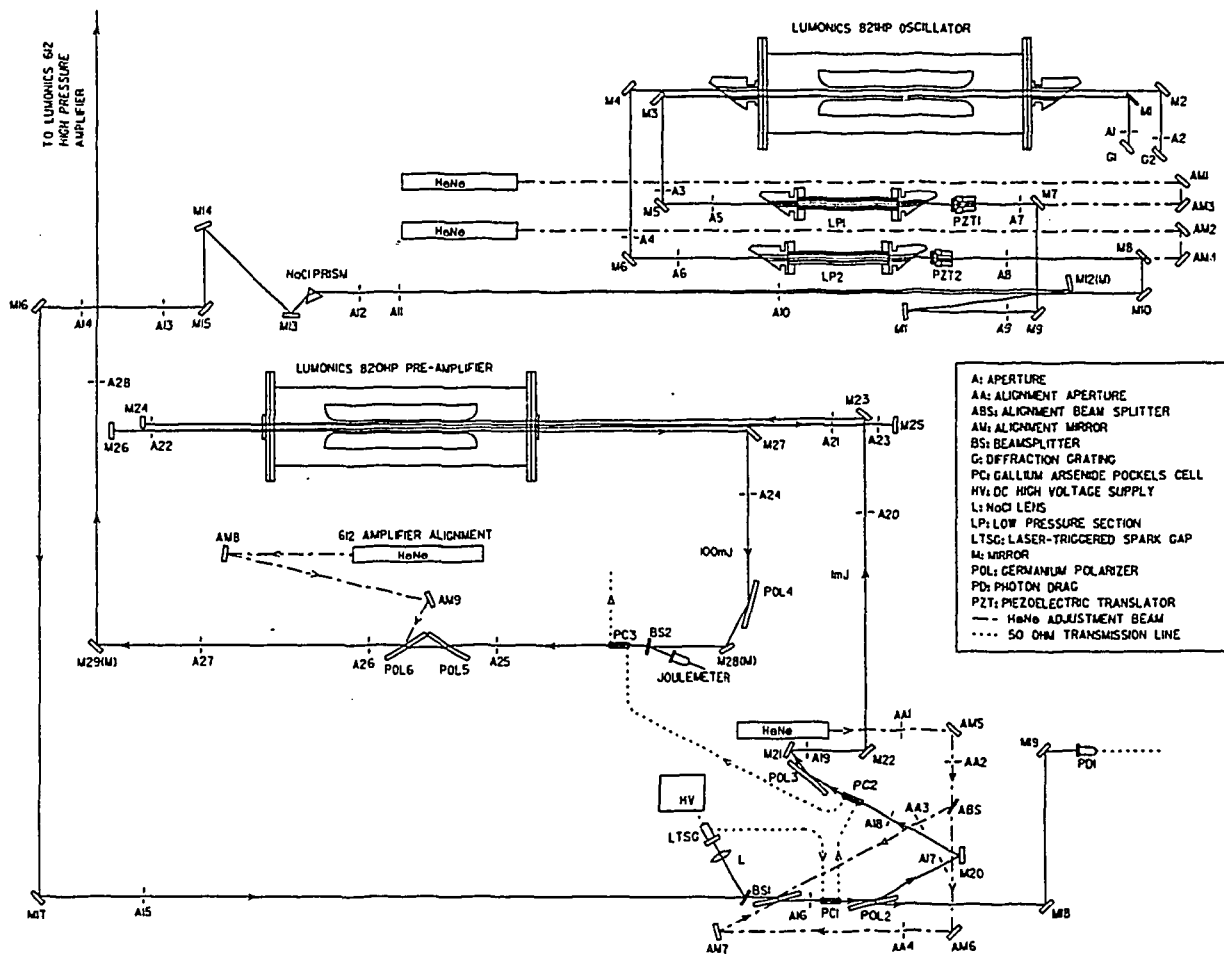
## IX. ACKNOWLEDGMENTS

We thank E.B. Selkirk, R.T.F. Bird, D.R. Proulx, J.E. Anderchek, R.J. Kelly, J.F. Weaver, and R.J. Bakewell for excellent technical support.

CANDU® is a registered trade mark of Atomic Energy of Canada Limited.

## X. REFERENCES

1. M.N. Rosenbluth and C.S. Liu, *Phys. Rev. Lett.* **29**, 701 (1972).
2. T. Tajima and J.M. Dawson, *Phys. Rev. Lett.* **43**, 267 (1979).
3. N.A. Ebrahim, *Physics in Canada* **45**, 178 (1989).
4. N.A. Ebrahim, *Research Trends in Physics*, Ed. A.M. Prokhorov, AIP (1992), pp. 310 - 351.
5. N.A. Ebrahim, *1992 Linac Conf. Proc.*, Ottawa, Atomic Energy of Canada Limited Report, AECL-10728, edited by C.R. Hoffmann (1992), p. 825.
6. N.A. Ebrahim, *J. Appl. Phys.* (1994).
7. A. Gondhalekar, E. Holzhauer and N.R. Heckenberg, *Phys. Lett.* **46A**, No. 3, 229 (1973).
8. S.C. Mehendale and R.G. Harrison, *Opt. Lett.* **10**, 603 (1985).
9. E.J. McLellan and F.J. Figueira, *Technical Digest of Topical Meeting on Inertial Confinement Fusion*, Paper Tu C11-1, San Diego (1978); E.J. McLellan and J.F. Figueira, *Rev. Sci. Instr.* **50**(10) (1979).
10. K.O. Tan, D.J. James, J.A. Nelson, N.H. Burnett and A.J. Alcock, *Rev. Sci. Instrum.* **51**, 776 (1980).



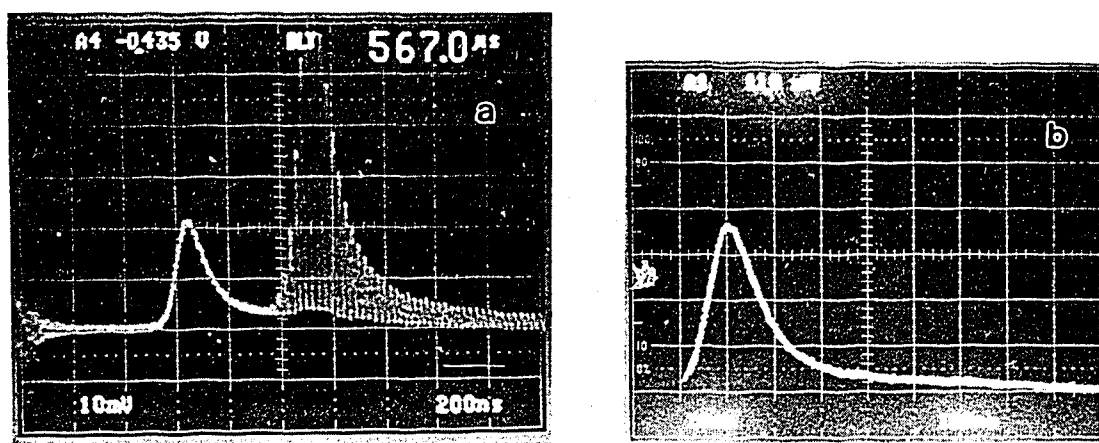
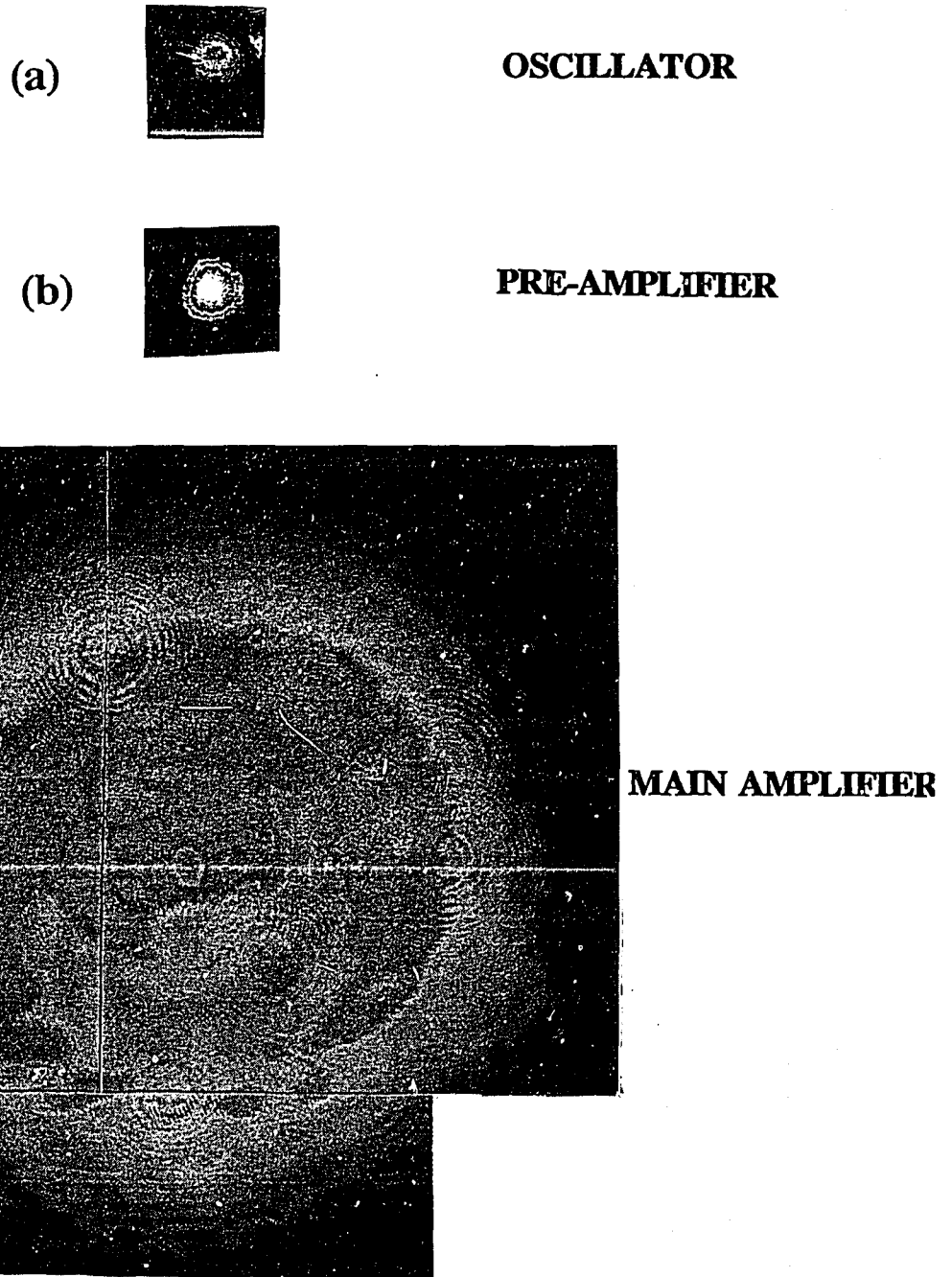


Figure 2. (a) Oscilloscope signals of laser emission at 10.59 and 10.25  $\mu\text{m}$  recorded simultaneously with a photon-drag detector. The low-pressure discharge in the 10.25  $\mu\text{m}$  laser cavity has been turned off in order to demonstrate the multi-mode output of the laser oscillator. (b) Synchronized laser output at 10.59 and 10.25  $\mu\text{m}$ .



**Figure 3.** (a) Signature of the oscillator beam recorded as a "burn-mark" on a sheet of unexposed polaroid film. (b) Signature of the pre-amplifier beam recorded as a "burn-mark" on a sheet of unexposed polaroid film. (c) Signature of the main laser beam recorded as a "burn-mark" on a sheet of unexposed polaroid film.

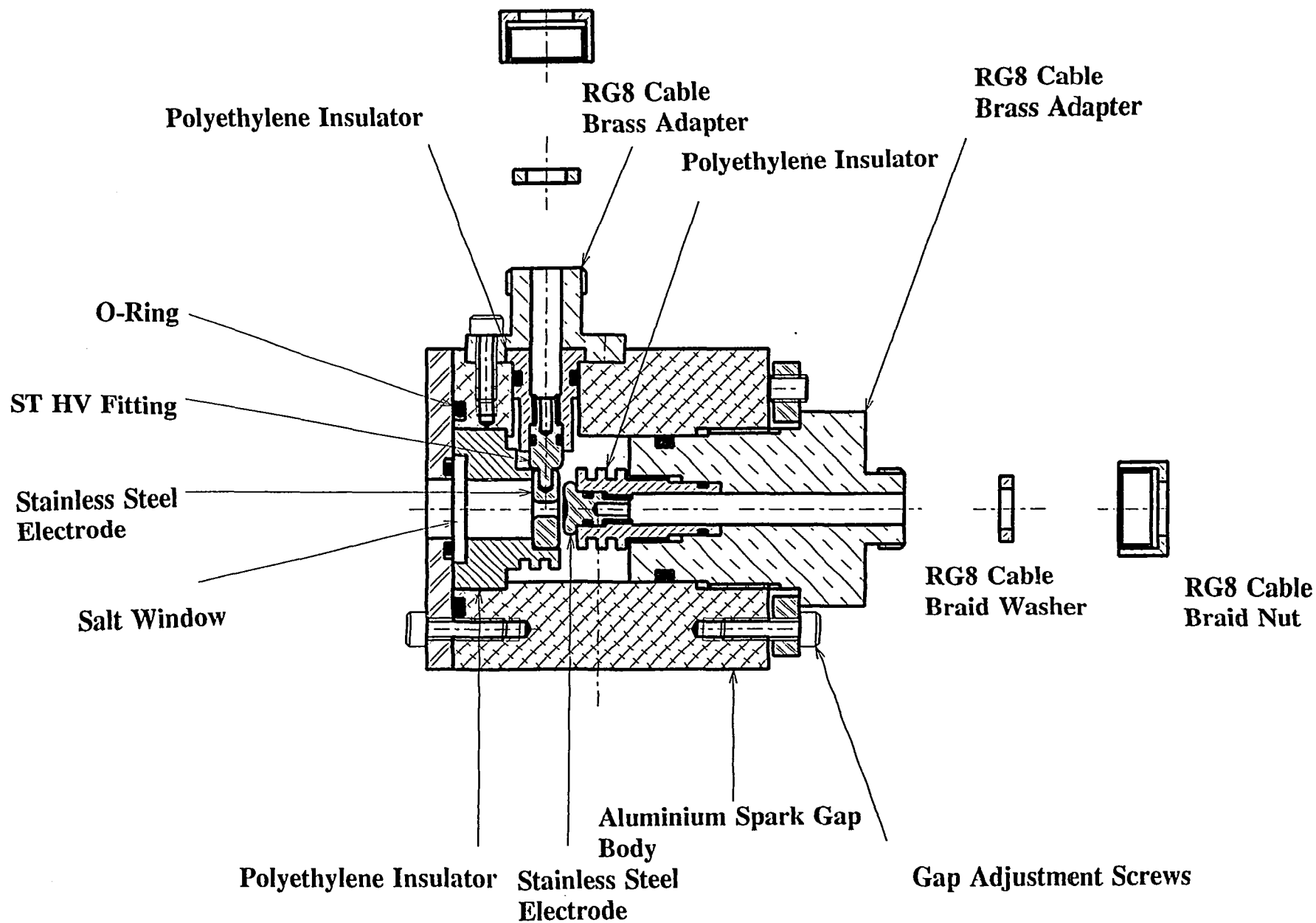


Fig. 4 Schematic of the laser-triggered spark gap (LTSG). The laser light enters the gap region from the left through the opening in the electrode.

## High-Pressure CO<sub>2</sub> Laser Amplifier (Lumonics 612)

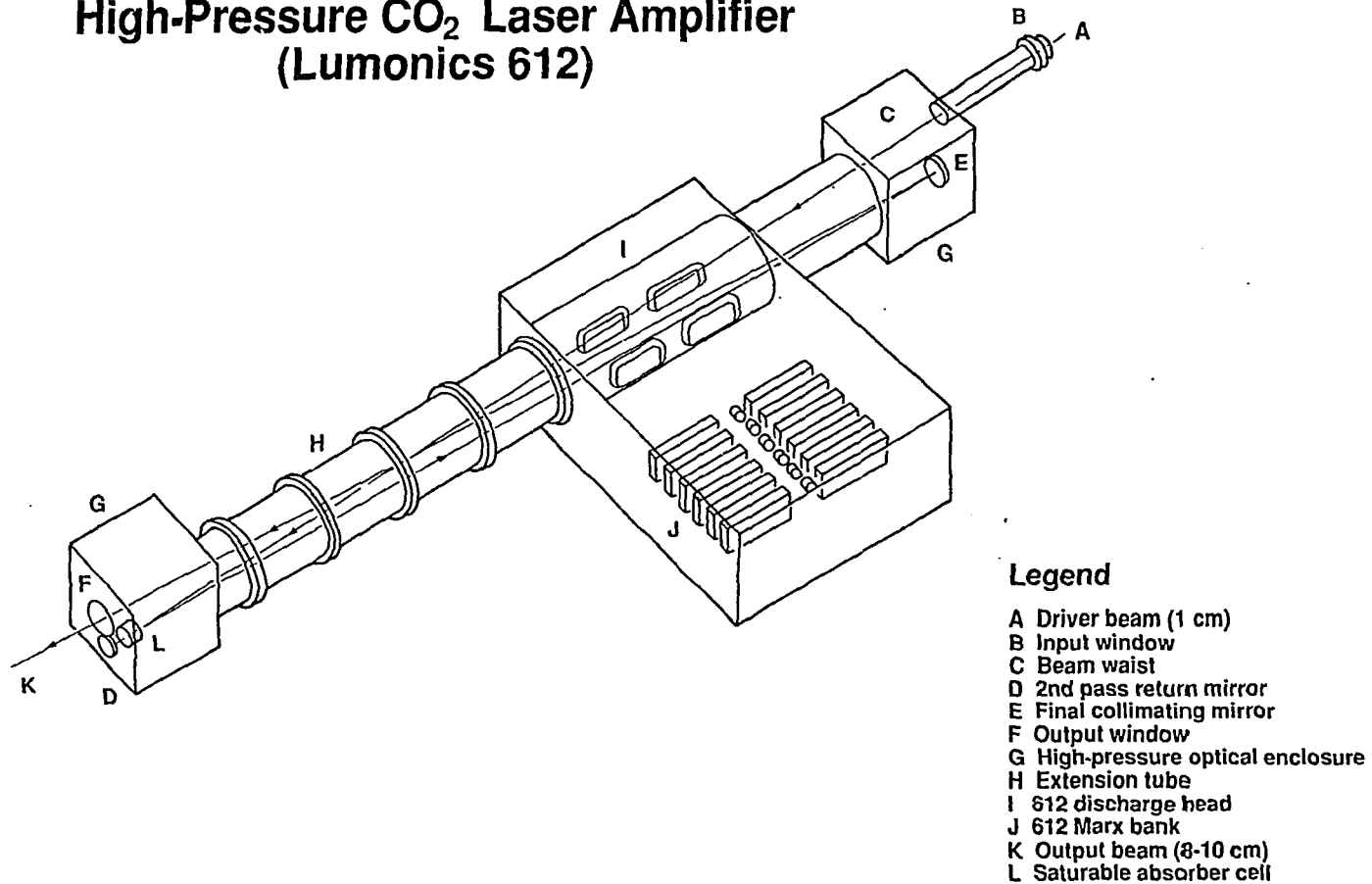
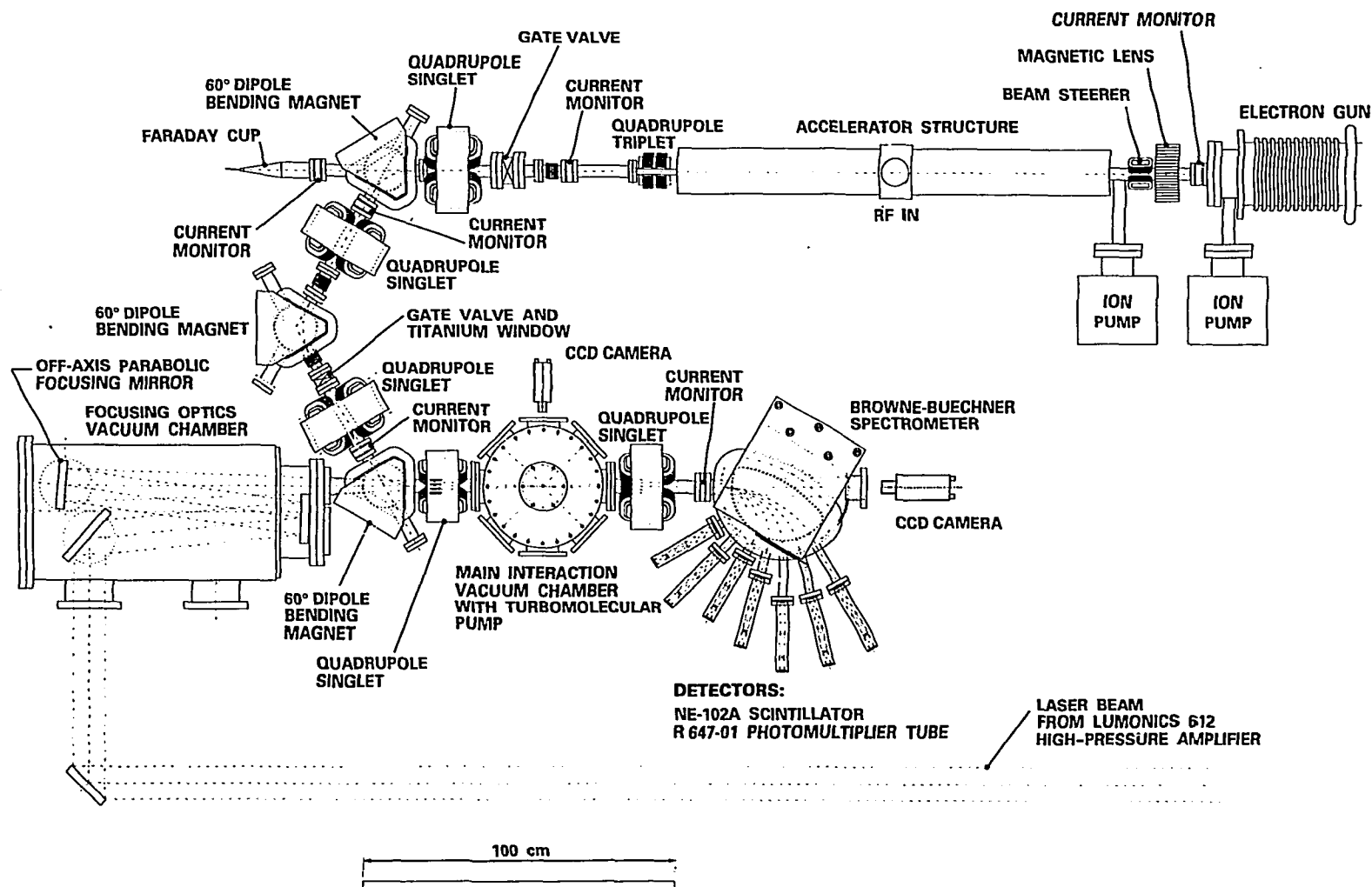
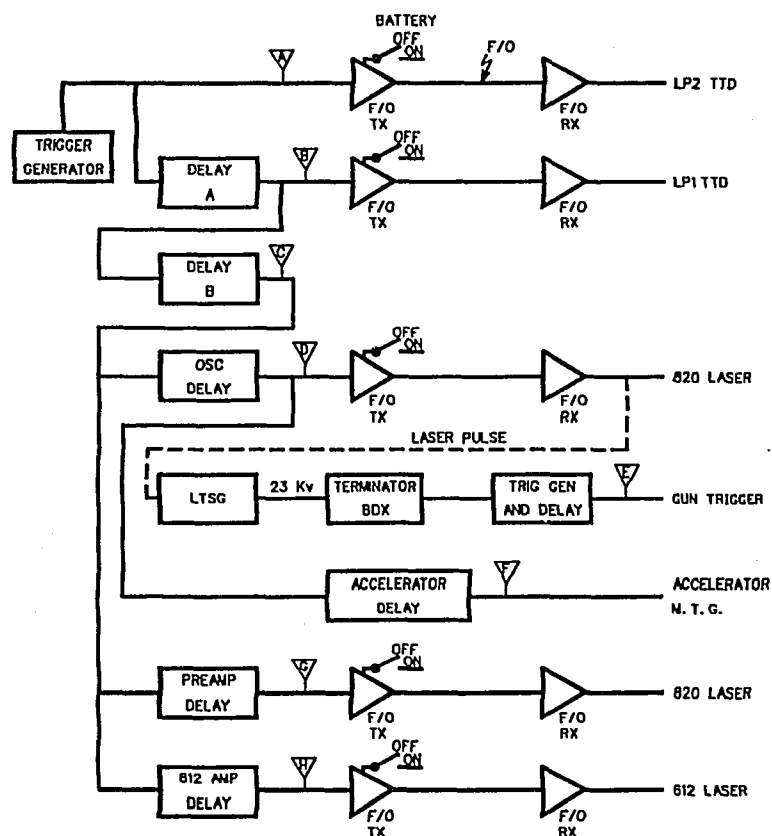


Figure 5. Schematic of the high-pressure CO<sub>2</sub> laser amplifier (LUMONICS 612).



**Figure 6.** Schematic of the experimental arrangement. The focussing and the main interaction vacuum chambers are shown.



LTSG - LASER-TRIGGERRED SPARK GAP  
TTD - TRIGGER TRANSFORMER DRIVER  
F/O - FIBRE OPTIC  
TX - TRANSMITTER

RX - RECEIVER  
LP - LOW-PRESSURE SMOOTHING TUBE  
OSC - OSCILLATOR  
MTG - MASTER-TIMING GENERATOR

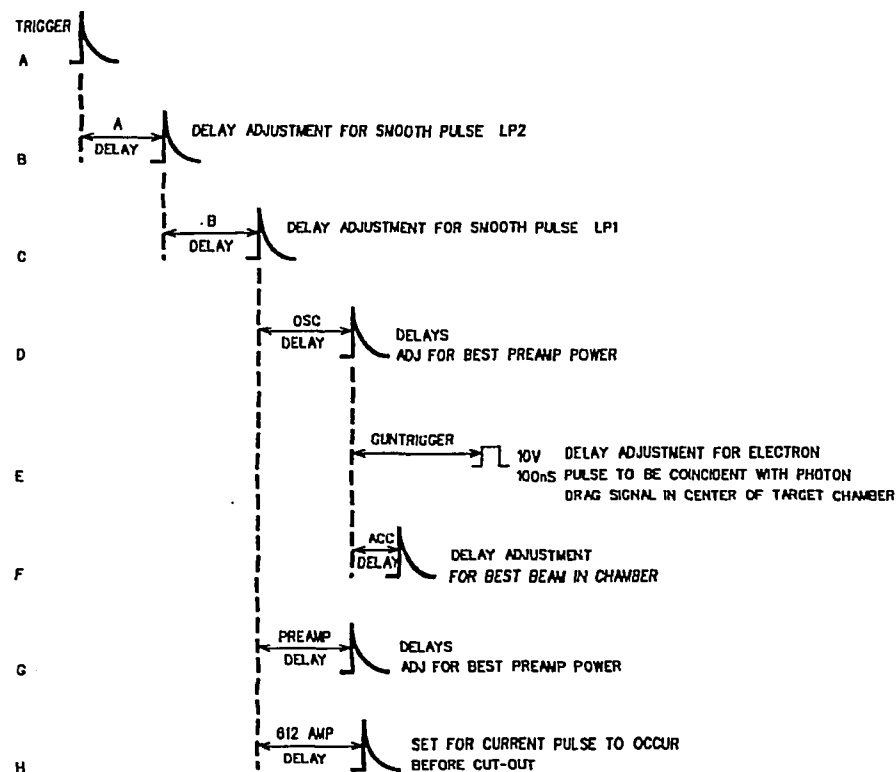


Figure 7. Schematic of the master timing generator to control the laser chain and to synchronize the laser pulse to the electron beam pulse.



RG8 Cable  
Braid Nut

RG8 Cable  
Adapter Flange

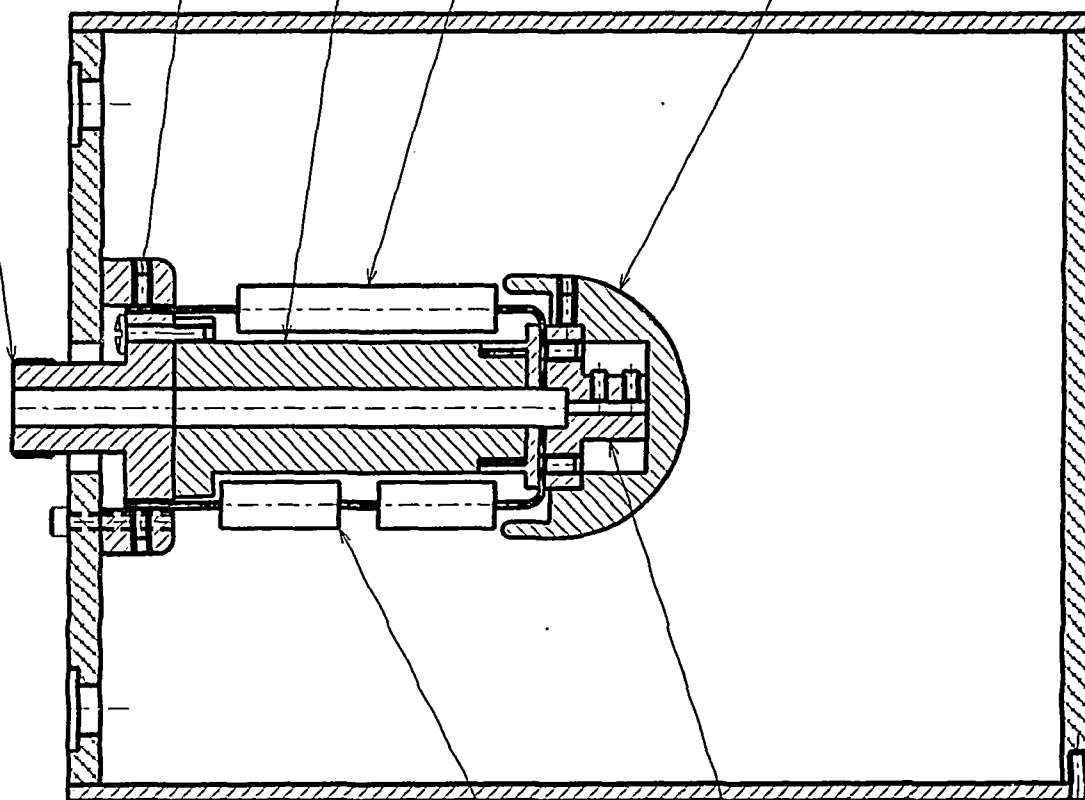
Nylon Insulator

Power Film Resistor  
(500  $\Omega$ , 12.5 watts)

Aluminium HV Termination

RG8 Cable  
Braid Washer

Hex Socket Set Screw



Power Film Resistor  
(50  $\Omega$  and 50 k $\Omega$ , 8 watts)

RG8 Cable  
Brass Adapter

High-Voltage Enclosure

Figure 8. Schematic of the high-voltage 50  $\Omega$  terminator and potential divider.

**Off-axis Parabolic Mirror**  
(Focal length = 125 cm, f/12.5)

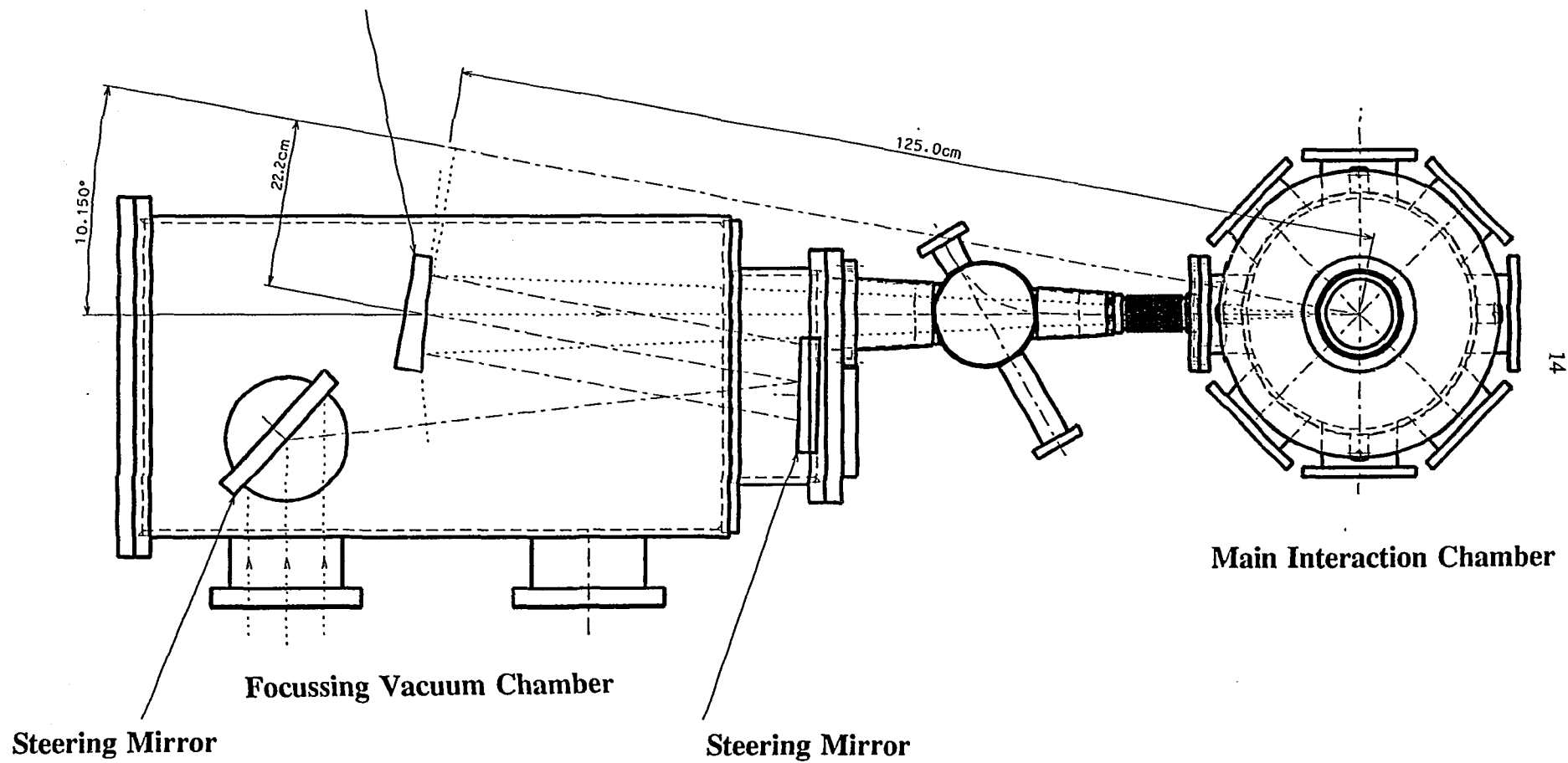


**Figure 9.** Schematic of the off-axis parabolic focussing mirror.

Cat. No. /No de cat.: CC2-11240E

ISBN 0-660-15910-4

ISSN 0067-0367

To identify individual documents in the series, we have assigned an AECL- number to each.

Please refer to the AECL- number when requesting additional copies of this document from:

Scientific Document Distribution Office (SDDO)

AECL Research

Chalk River, Ontario

Canada K0J 1J0

Fax: (613) 584-1745

Tel.: (613) 584-3311  
ext. 4623

Price: A

Pour identifier les rapports individuels faisant partie de cette serie, nous avons affecté un numéro AECL- à chacun d'eux.

Veuillez indiquer le numéro AECL- lorsque vous demandez d'autres exemplaires de ce rapport au:

Service de Distribution des Documents Officiels

EACL Recherche

Chalk River (Ontario)

Canada K0J 1J0

Fax: (613) 584-1745

Tél.: (613) 584-3311  
poste 4623

Prix: A

